A General Charting Scheme For Monitoring Serially Correlated Data With Short-Memory Dependence and Nonparametric Distributions

Wendong Li[1] and Peihua Qiu[2]
[1]School of Statistics, East China Normal University, Shanghai, China
[2]Department of Biostatistics, University of Florida, Gainesville, USA

Abstract

Traditional statistical process control charts are based on the assumptions that process observations are independent and identically normally distributed when the related process is in-control (IC). In recent years, it has been demonstrated in the literature that these traditional control charts are unreliable to use when their model assumptions are violated. Several new research directions have been developed, in which new control charts have been proposed for handling cases when the IC process distribution is nonparametric with a reasonably large IC data, when the IC process distribution is unknown with a small IC data, or when the process observations are serially correlated. However, existing control charts in these research directions can only handle one or two cases list above, and they cannot handle all cases simultaneously. In most applications, it is typical that the IC process distribution is unknown and hard to be described by a parametric form, the process observations are serially correlated with a short-memory dependence, and only a small to moderate IC dataset is available. This paper suggests an effective charting scheme to tackle such a challenging and general process monitoring problem. Numerical studies show that it works well in different cases considered.

Key Words: Data correlation; In-control data; Nonparametric; Online monitoring; Self-starting chart; Statistical process control.

1 Introduction

Statistical process control (SPC) charts have broad applications in manufacturing industries, disease surveillance, environmental monitoring, and more. Traditional SPC charts are based on the assumptions that process observations are independent and identically distributed (i.i.d.) and follow a parametric distribution (e.g., normal) when the related process

is in-control (IC). See systematic descriptions in books such as Hawkins and Olwell (1998), Montgomery (2012), and Qiu (2014). In practice, these assumptions are rarely valid, and it has been well demonstrated in the literature that the traditional SPC charts are unreliable to use when their model assumptions are violated (cf., Chakraborti et al. 2015, Qiu 2018). This paper tries to develop a general charting scheme for process monitoring applications in which all assumptions mentioned above might be invalid.

In the SPC literature, it has been discussed intensively that the IC performance of traditional SPC charts based on a parametric distribution assumption could be far from what would be expected in cases when such a parametric distribution assumption is invalid. More specifically, the IC average run length (ARL) value could be substantially different from a nominal value in such cases. To overcome this limitation of traditional SPC charts, nonparametric SPC has become an active research area, and many nonparametric SPC charts have been developed recently. Most nonparametric SPC charts are constructed based on the ranking/ordering information in the observed data (e.g., Chakraborti et al. 2001, Li et al. 2013, Mukherjee et al. 2013, Qiu and Hawkins 2001, 2003, Zou et al. 2012). Some others are based on data categorization and categorical data analysis (e.g., Li 2017, Qiu 2008, Qiu and Li 2011). For a recent overview, see Qiu (2018). In cases when process observations are serially correlated, it is demonstrated in Hawkins and Olwell (1998) and Qiu (2014) that the data correlation should not be ignored. Otherwise, the related control charts are unreliable. To overcome that limitation, a commonly used strategy in the literature is to fit a parametric time series model and then apply a control chart to the residuals of the fitted model (e.g., Apley and Tsung 2002, Loredo et al. 2002, Wardell et al. 1994). However, it has been shown that process monitoring based on this idea is unrobust to the assumed parametric time series model (Apley and Lee 2003, 2008). Thus, some modifications have been suggested in papers, such as Lee and Apley (2011), Qiu et al. (2019) and Zhang (1998). Another strategy for handling serially correlated data is to adjust control limits of conventional control charts (e.g., Runger 2002, Vermaat et al. 2008). In most methods mentioned above for handling cases with nonparametric process distributions and/or serially correlated observed data, a large IC dataset is often needed for estimating IC parameters or setting up the control charts to have a reliable IC performance. In some applications, such a large IC dataset may not be available. To overcome this difficulty, Hawkins (1987) suggested the idea of self-starting process monitoring, by which observations collected during online monitoring were combined with the existing IC data if no signal was given at the current time point. Thus, a self-starting

control chart only requires a handful of IC observations before online monitoring and the IC sample size would keep increasing during process monitoring.

In industrial applications, it is often the case that the IC process distribution is unknown and inappropriate to be described by a parametric form, the process observations are serially correlated with a short-memory dependence but the serial data correlation cannot be described by a parametric time series model, and a large IC dataset is unavailable. See Section 4 for a real-data example. The existing methods discussed above try to address one or two such issues. But, to make a SPC chart most useful to industrial applications, it should be able to tackle all of them properly. So far, we cannot find a single method to achieve that challenging goal yet, and this paper aims to fill the gap. In this paper, we propose a general charting scheme for monitoring serially correlated process observations with short-memory data dependence and unknown process distributions. This chart does not require any parametric form to describe the process IC distribution. It does not require a parametric time series model either for describing serial data dependence. All it needs is a small to moderate IC dataset for providing initial estimates of certain IC parameters. Then, the estimates of these IC parameters will be updated recursively in the proposed chart for improving their accuracy. So, the proposed control chart is a self-starting nonparametric chart which can accommodate short-memory data dependence. As far as we know, it is the first chart of this type in the literature. The remaining part of the paper is organized as follows. Our proposed method is described in detail in Section 2. Its numerical performance is investigated in Section 3. A real-data application is discussed in Section 4. Then, several remarks conclude the paper in Section 5.

2 Proposed General Charting Scheme

We focus on Phase II online monitoring of process observations $X_1, X_2, \ldots, X_n$, where $n \geq 1$ is the current time point during process monitoring. The IC process distribution is assumed to be unknown. All we have about the IC process distribution is a small to moderate set of IC observations $\boldsymbol{X}_{IC} = \{X_{-m_0+1}, X_{-m_0+2}, \ldots, X_0\}$ with the size m_0, collected before Phase II online monitoring. The process observations could be serially correlated. Because it is reasonable to assume that the process under consideration in many industrial applications is covariance stationary when it is IC, we assume that $\gamma(s) = \text{Cov}(X_i, X_{i+s})$ does not depend

on i, for all $i \geq 1$. Namely, the correlation between two observations X_i and X_{i+s} does not change if the distance in their observation indices, s, keeps a constant. Furthermore, in most applications it is reasonable to assume that the correlation between X_i and X_{i+s} would decrease when s increases. Consequently, when two observations are sufficiently apart in observation times, the correlation between them is negligible. Therefore, in this paper, we assume that $\gamma(s) = 0$ when $s \geq b_{max}$, where $b_{max} \geq 1$ is an integer.

2.1 Initial estimation from the IC data

From the IC data $\boldsymbol{X}_{IC}$ of size m_0, we first calculate initial estimates of the IC mean μ and IC covariances $\{\gamma(s), 0 \leq s \leq b_{max}\}$. Because the IC process distribution is unknown, moment estimates of these parameters are reasonable to use, which are defined as follows:

$$\begin{aligned} \widehat{\mu}^{(0)} &= \frac{1}{m_0} \sum_{i=-m_0+1}^{0} X_i, \\ \widehat{\gamma}^{(0)}(s) &= \frac{1}{m_0 - s} \sum_{i=-m_0+1}^{-s} \left(X_{i+s} - \widehat{\mu}^{(0)}\right)\left(X_i - \widehat{\mu}^{(0)}\right), \text{ for } s = 0, 1, \ldots, b_{max}. \end{aligned}$$

Then, the IC data can be de-correlated recursively by the following algorithm that is based on the Cholesky decomposition of the covariance matrices:

- When $i = -m_0 + 1$, define the de-correlated and standardized observation to be $X_i^* = (X_i - \widehat{\mu}^{(0)})/\sqrt{\widehat{\gamma}^{(0)}(0)}$, and let $b = 1$.
- For $i > -m_0 + 1$, let the estimated covariance matrix be

$$\widehat{\boldsymbol{\Sigma}}_{\boldsymbol{i,i}} = \begin{pmatrix} \widehat{\gamma}^{(0)}(0) & \cdots & \widehat{\gamma}^{(0)}(b) \\ \vdots & \ddots & \vdots \\ \widehat{\gamma}^{(0)}(b) & \cdots & \widehat{\gamma}^{(0)}(0) \end{pmatrix} = \begin{pmatrix} \widehat{\boldsymbol{\Sigma}}_{\boldsymbol{i-1,i-1}} & \widehat{\boldsymbol{\sigma}}_{\boldsymbol{i-1}} \\ \widehat{\boldsymbol{\sigma}}_{\boldsymbol{i-1}}^{\boldsymbol{T}} & \widehat{\gamma}^{(0)}(0), \end{pmatrix},$$

  where $\widehat{\boldsymbol{\sigma}}_{\boldsymbol{i-1}} = (\widehat{\gamma}^{(0)}(b), \ldots, \widehat{\gamma}^{(0)}(1))^T$. Define the ith de-correlated and standardized observation to be

$$X_i^* = \frac{X_i - \widehat{\mu}^{(0)} - \widehat{\boldsymbol{\sigma}}_{\boldsymbol{i-1}}^{\boldsymbol{T}} \widehat{\boldsymbol{\Sigma}}_{\boldsymbol{i-1,i-1}}^{-1} \boldsymbol{e}_{\boldsymbol{i-1}}}{\widehat{d}_i},$$

  where $\widehat{d}_i^2 = \widehat{\gamma}^{(0)}(0) - \widehat{\boldsymbol{\sigma}}_{\boldsymbol{i-1}}^{\boldsymbol{T}} \widehat{\boldsymbol{\Sigma}}_{\boldsymbol{i-1,i-1}}^{-1} \widehat{\boldsymbol{\sigma}}_{\boldsymbol{i-1}}$, and $\boldsymbol{e}_{\boldsymbol{i-1}} = (X_{i-b} - \widehat{\mu}^{(0)}, \ldots, X_{i-1} - \widehat{\mu}^{(0)})^T$. Let $b = \min(b + 1, b_{max})$ and $i = i + 1$. Repeat this step until $i > 0$.

Theoretically speaking, if $\widehat{\mu}^{(0)}$ and $\{\widehat{\gamma}^{(0)}(s), 0 \le s \le b_{max}\}$ were the true IC process mean and covariances, then it can be checked that the de-correlated and standardized observations $\{X_i^*, i = -m_0+1, \ldots, 0\}$ are uncorrelated and each has mean 0 and variance 1. See a related discussion in Li and Qiu (2016), where the Cholesky decomposition is used in the context of dynamic process monitoring. Because the sample size m_0 of the IC data could be small, the accuracy of $\widehat{\mu}^{(0)}$ and $\{\widehat{\gamma}^{(0)}(s), 0 \le s \le b_{max}\}$ in estimating the IC process mean and covariances may be limited. According to Box et al. (2013), these estimates might be reliable only when $m_0 \ge 50$ and $s \le m_0/4$. To overcome this limitation, a self-starting control chart is suggested below for online process monitoring, in which the estimates of the IC process mean and covariances are updated sequentially.

2.2 Self-starting monitoring of correlated data with nonparametric distributions

To monitor the correlated Phase II observations $X_1, X_2, \ldots$ properly, we first sequentially de-correlate and standardize them so that conventional control charts can be applied. Let n be the current time point. Then, X_n needs to be de-correlated with all previous observations at time n, which will be computing intensive, especially in cases when n is large. To reduce the computing burden, we would like to make use of the restarting mechanism of the CUSUM chart that previous observations up to the current time point n can be ignored in subsequent process monitoring if all available observations suggest that there is no evidence of a process distributional shift. More specifically, we will use the spring length T_n first suggested in Chatterjee and Qiu (2009), defined as the number of observations between the current time point n and the last time point at which a CUSUM charting statistic is zero. By using the idea of spring length, all observations collected before the time $n - T_n$ can all be ignored in subsequent process monitoring, because they do not provide evidence of process distributional shift and their inclusion can only make the chart less sensitive to a future shift. Thus, we only need to de-correlate the current observation X_n with the previous T_{n-1} observations and ignore all other history data. The sequentially de-correlated data are denoted as $X_1^*, X_2^*, \ldots$, and more details will be given below.

Second, the estimates of the IC parameters μ and $\{\gamma(s), 0 \le s \le b_{max}\}$ should be updated at time n if the related control chart does not give a signal at time n and thus the observation

X_n can be combined with the IC data. The recursive formulas for updating these estimates are given below: for $n \geq 1$ and $0 \leq s \leq b_{max}$,

$$\widehat{\mu}^{(n)} = \frac{1}{m_0+n} X_n + \frac{m_0+n-1}{m_0+n} \widehat{\mu}^{(n-1)}, \tag{1}$$

$$\widehat{\gamma}^{(n)}(s) = \frac{1}{m_0+n-s} (X_n - \widehat{\mu}^{(n)})(X_{n-s} - \widehat{\mu}^{(n)}) + \frac{m_0+n-s-1}{m_0+n-s} \widehat{\gamma}^{(n-1)}(s). \tag{2}$$

If the original observations $X_1, X_2, \ldots$ are normally distributed, then the de-correlated and standardized observations $X_1^*, X_2^*, \ldots$ will be roughly i.i.d. and normally distributed. In such cases, the conventional charts, such as the regular CUSUM and EWMA charts, should be appropriate to apply to the de-correlated and standardized observations for process monitoring. However, in practice, the IC distribution of the original observations could be far away from a normal distribution (e.g., skewed or heavy-tailed). In such cases, the conventional charts would be unreliable and their results could be misleading if they are applied to the de-correlated and standardized observations directly, because the distribution of the de-correlated observations could be far away from a normal distribution (cf., Qiu 2014, Chapters 8 and 9). For this reason, we suggest using the following nonparametric control chart based on data categorization, modified from the one in Qiu and Li (2011) where a univariate nonparametric CUSUM chart was proposed based on data categorization when process observations are assumed independent and a large IC data are assumed available for estimating IC parameters (i.e., self-starting chart was not discussed there).

Let $I_1 = (-\infty, q_1], I_2 = (q_1, q_2], \ldots, I_p = (q_{p-1}, \infty)$ be a partition of the real line, with $-\infty < q_1 < q_2 < \cdots < q_{p-1} < \infty$ being the $p-1$ boundary points of the partitioning intervals. Define $Y_{n,l} = I(X_n^* \in I_l)$, for $l = 1, 2, \ldots, p$, and $\boldsymbol{Y}_n = (Y_{n,1}, Y_{n,2}, \ldots, Y_{n,p})^T$. Then, $\boldsymbol{Y}_n$ has one component being 1 and the remaining being 0, and the index of the component being 1 is the index of the partitioning interval that contains X_n^*. Let $\boldsymbol{f}^{(0)} = (f_1^{(0)}, f_2^{(0)}, \ldots, f_p^{(0)})^T$ be the IC distribution of $\boldsymbol{Y}_n$. Then, it is not difficult to check that if there is a location or scale shift from the IC distribution of the original observations, the distribution of the discretized data $\boldsymbol{Y}_n$ will change from $\boldsymbol{f}^{(0)}$. So, detection of a location or scale shift in the distribution of the original data can be achieved by detecting a distributional shift in the discretized data. According to Agresti (2012), the distributional shift detection will be most effective if we choose $\boldsymbol{f}^{(0)} = (1/p, 1/p, \ldots, 1/p)^T$. In such cases, q_l, for $l = 1, 2, \ldots, p-1$, can be estimated by the (l/p)th sample quantile of the decorrelated IC dataset. Then, the suggested nonparametric CUSUM chart is defined as follows. Let $\boldsymbol{S}_0^{obs} = \boldsymbol{S}_0^{exp} = \boldsymbol{0}$ be two

$p \times 1$ column vectors, and

$$\begin{cases} \boldsymbol{S}_n^{obs} = \boldsymbol{S}_n^{exp} = \boldsymbol{0}, & \text{if } D_n \le k \\ \boldsymbol{S}_n^{obs} = (\boldsymbol{S}_{n-1}^{obs} + \boldsymbol{Y}_n)(D_n - k)/D_n, & \text{if } D_n > k \\ \boldsymbol{S}_n^{exp} = (\boldsymbol{S}_{n-1}^{exp} + \boldsymbol{f}^{(0)})(D_n - k)/D_n, & \text{if } D_n > k, \end{cases}$$

where

$$D_n = \left\{(\boldsymbol{S}_{n-1}^{obs} - \boldsymbol{S}_{n-1}^{exp}) + (\boldsymbol{Y}_n - \boldsymbol{f}^{(0)})\right\}^T (diag(\boldsymbol{S}_{n-1}^{obs} + \boldsymbol{f}^{(0)}))^{-1} \left\{(\boldsymbol{S}_{n-1}^{obs} - \boldsymbol{S}_{n-1}^{exp}) + (\boldsymbol{Y}_n - \boldsymbol{f}^{(0)})\right\},$$

and k is an allowance parameter. Define the charting statistic to be

$$C_n = (\boldsymbol{S}_n^{obs} - \boldsymbol{S}_n^{exp})^T (diag(\boldsymbol{S}_n^{exp}))^{-1} (\boldsymbol{S}_n^{obs} - \boldsymbol{S}_n^{exp}). \tag{3}$$

Then, the chart gives a signal if

$$C_n > h, \tag{4}$$

where $h > 0$ is a control limit. In the above expressions, $\boldsymbol{S}_{n-1}^{obs} + \boldsymbol{Y}_n$ tends to denote the cumulative observed counts of the de-correlated observations in the p partitioning intervals, and $\boldsymbol{S}_{n-1}^{exp} + \boldsymbol{f}^{(0)}$ tends to denote the cumulative expected counts when the process is IC. The charting statistic C_n in (3) measures the difference between the observed and expected counts. By using similar arguments to Appendix C in Qiu and Hawkins (2001) where a multivariate nonparametric control chart was proposed based on anti-ranks of multivariate observations, we can check that $C_n = \max(0, D_n - k)$. So, the charting statistic C_n repeatedly restart at 0 when there is little evidence of a distributional shift in $\boldsymbol{Y}_n$ (i.e., when $D_n \le k$). This restarting mechanism would make the chart (3)-(4) effective in shift detection, as discussed in the literature about the conventional CUSUM chart (cf., Qiu 2014, Chapter 4).

In the above CUSUM chart (3)-(4), the (l/p)th sample quantiles, for $l = 1, 2, \ldots, p-1$, need to be calculated from the IC dataset. At the current time point n, if the chart (3)-(4) does not give a signal, then X_n can be combined with the previous IC dataset, and these sample quantiles should be updated recursively to improve their accuracy in estimating the corresponding population parameters. To be more specific, let the (l/p)th sample quantiles from the de-correlated and standardized original IC data $\boldsymbol{X}_{IC}^* = \{X_{-m_0+1}^*, X_{-m_0+2}^*, \ldots, X_0^*\}$ be $\widehat{q}_l^{(0)}$, the (l/p)th sample quantiles from the combined IC data up to the previous time point $n-1$ be $\widehat{q}_l^{(n-1)}$, and the de-correlated and standardized process observations by time $n-1$ that are immediately before and after $\widehat{q}_l^{(n-1)}$ in the ordered data be $X_{l,b}^*$ and $X_{l,a}^*$,

respectively, for $l = 1, 2, \ldots, p-1$. Then, the (l/p)th sample quantiles by time n is one of $\{X^*_{l,b}, \widehat{q}_l^{(n-1)}, X^*_{l,a}\}$, depending on whether $l(m_0+n-1)/p$ and $l(m_0+n)/p$ specify different observations at times $n-1$ and n and which partitioning interval the new de-correlated and standardized observation X^*_n belongs to.

The proposed control chart for monitoring serially correlated data with unknown and nonparametric IC process distribution can then be summarized below.

- When $n = 1$, define the standardized observation to be $X^*_n = (X_n - \widehat{\mu}^{(0)})/\sqrt{\widehat{\gamma}^{(0)}(0)}$. Calculate the charting statistic C_n using (3) in which the $p-1$ boundary points of the partitioning intervals are chosen to be $\widehat{q}_l^{(0)}$, for $l = 1, 2, \ldots, p-1$. The chart gives a signal if (4) is true.

- When $n > 1$, if $T_{n-1} = 0$, then define $X^*_n = (X_n - \widehat{\mu}^{(n-1)})/\sqrt{\widehat{\gamma}^{(n-1)}(0)}$. Otherwise, let

$$\widehat{\boldsymbol{\Sigma}}_{\boldsymbol{n,n}} = \begin{pmatrix} \widehat{\gamma}^{(n-1)}(0) & \cdots & \widehat{\gamma}^{(n-1)}(T_{n-1}) \\ \vdots & \ddots & \vdots \\ \widehat{\gamma}^{(n-1)}(T_{n-1}) & \cdots & \widehat{\gamma}^{(n-1)}(0) \end{pmatrix} = \begin{pmatrix} \widehat{\boldsymbol{\Sigma}}_{\boldsymbol{n-1,n-1}} & \widehat{\boldsymbol{\sigma}}_{\boldsymbol{n-1}} \\ \widehat{\boldsymbol{\sigma}}^{\boldsymbol{T}}_{\boldsymbol{n-1}} & \widehat{\gamma}^{(n-1)}(0), \end{pmatrix},$$

  where $\widehat{\boldsymbol{\sigma}}_{\boldsymbol{n-1}} = (\widehat{\gamma}^{(n-1)}(T_{n-1}), \ldots, \widehat{\gamma}^{(n-1)}(1))^T$. Then, define

$$X^*_n = \frac{X_n - \widehat{\mu}^{(n-1)} - \widehat{\boldsymbol{\sigma}}^{\boldsymbol{T}}_{\boldsymbol{n-1}} \widehat{\boldsymbol{\Sigma}}^{-1}_{\boldsymbol{n-1,n-1}} \boldsymbol{e}_{\boldsymbol{n-1}}}{\widehat{d}_n},$$

  where $\widehat{d}_n^2 = \widehat{\gamma}^{(n-1)}(0) - \widehat{\boldsymbol{\sigma}}^{\boldsymbol{T}}_{\boldsymbol{n-1}} \widehat{\boldsymbol{\Sigma}}^{-1}_{\boldsymbol{n-1,n-1}} \widehat{\boldsymbol{\sigma}}_{\boldsymbol{n-1}}$, and $\boldsymbol{e}_{\boldsymbol{n-1}} = (X_{n-T_{n-1}} - \widehat{\mu}^{(n-1)}, \ldots, X_{n-1} - \widehat{\mu}^{(n-1)})^T$. Then, we calculate C_n by (3) in which the $p-1$ boundary points of the partitioning intervals are chosen to be $\widehat{q}_l^{(n-1)}$, for $l = 1, 2, \ldots, p-1$. If $C_n = 0$, then define $T_n = 0$. Otherwise, define $T_n = \min(T_{n-1} + 1, b_{max})$. The quantities $\widehat{\mu}^{(n)}$, $\{\widehat{\gamma}^{(n)}(s), 0 \le s \le b_{max}\}$ and $\{\widehat{q}_l^{(n)}, l = 1, 2, \ldots, p-1\}$ can be calculated by the recursive algorithms described above. The chart gives a signal when (4) is true.

This chart is called G-CUSUM chart hereafter, where the first letter "G" represents "general". From the above description, it can be seen that G-CUSUM combines the ideas of nonparametric process monitoring based on data categorization, recursive estimation of IC parameters under a self-starting monitoring framework, and data decorrelation. In the literature, there are existing methods using one of these ideas. But, G-CUSUM chart is the first one that combines all of them in a dynamic and efficient way so that it can handle a wide variety of process monitoring problems.

2.3 Practical guidelines on parameter selection

On selection of m_0: The proposed self-starting control chart G-CUSUM requires an IC dataset $\boldsymbol{X}_{IC}$ of the size m_0. If m_0 is chosen too small, then process monitoring in the initial stage may not be reliable because the estimates of the IC parameters $\mu, \{\gamma(s), 0 \le s \le b_{max}\}$ and $\{q_l, l = 1, 2, \ldots, p-1\}$ may not be reliable. In such cases, if a short-run change occurs, then it is likely to be missed. Numerical results given in Section 3 show that (i) the IC performance of the chart G-CUSUM is reliable when $m_0 \ge 200$, (ii) its OC performance for detecting moderate to large shifts is good when $m_0 \ge 200$, and (iii) its OC performance for detecting small shifts is reasonably good when $m_0 \ge 500$.

On selection of h: In the CUSUM chart (3)-(4), the allowance constant k is usually pre-specified together with the ARL_0 value. Then, the control limit h should be chosen to reach the given ARL_0 value. To this end, it can be determined easily by a numerical algorithm described below. First, choose an initial value for h (e.g., $h = 10$). Then, compute the actual ARL_0 value based on a large number (e.g. 10,000) of replicated simulation runs, in each of which the IC multinomial observations $\boldsymbol{Y}_n$ are sequentially generated from the IC distribution $\boldsymbol{f}^{(0)} = (1/p, ..., 1/p)^T$. If the computed ARL_0 value is smaller than the given ARL_0 value, then increase the value of h. Otherwise, choose a smaller h value. The above process is repeated until the given ARL_0 value is reached within a desired precision. In this process, some numerical searching schemes, such as the bisection search, can be applied (cf., Qiu 2008).

On selection of b_{max}: Serial data correlation is assumed homogeneous in this paper and two observations are assumed uncorrelated if they are at least $b_{max} + 1$ time points apart. In applications, b_{max} is often unknown and it needs to be pre-specified to use the proposed method. Of course, selection of b_{max} is usually application specific. Intuitively, b_{max} should be chosen as large as possible. But, as pointed out in Section 2.1, the estimates of $\{\gamma(s), 0 \le s \le b_{max}\}$ may not be reliable if b_{max} is chosen too large, especially in the initial period of process monitoring. From our numerical experience, performance of the proposed chart does not change much when $10 \le b_{max} \le 20$, and the results could be worse in some cases when b_{max} is chosen larger than 20. In Section 3, we will present many numerical results of G-CUSUM when $b_{max} = 10$. This value has been shown to work well for a wide range of serial data correlation structures, and it is recommended here.

3 Numerical Studies

We present some simulation results in this section about the performance of the proposed control chart G-CUSUM. For comparison purposes, the following four alternative methods are also considered, which well represent the current process control strategies in the literature for serially correlated data with unknown nonparametric IC distributions.

- Self-starting CUSUM, denoted as SS-CUSUM: The original self-starting CUSUM suggested by Hawkins (1987) was designed for cases when the process observations are assumed independent, the IC process distribution is assumed normal, and the IC process mean μ and variance σ^2 were assumed unknown. Then, the two unknown parameters μ and σ^2 can be estimated by $\widehat{\mu}^{(n)}$ and $\widehat{\gamma}^{(n)}(0)$ (cf., (1)-(2)), respectively, for monitoring the process at time n. Let

$$Z_n = \mathbf{\Phi}^{-1}\left[\mathbf{\Upsilon}_{m_0+n-2}\left(\sqrt{\frac{m_0+n-1}{m_0+n}} \times \frac{X_n - \widehat{\mu}^{(n)}}{\sqrt{\widehat{\gamma}^{(n)}(0)}}\right)\right],$$

  where $\mathbf{\Phi}$ is the cumulative distribution function (cdf) of the $N(0,1)$ distribution, $\mathbf{\Phi}^{-1}$ is its inverse, and $\mathbf{\Upsilon}_{m_0+n-2}$ is the cdf of the $t(m_0+n-2)$ distribution. Then, the charting statistics of SS-CUSUM are defined to be: for $n \geq 1$,

$$C^+_{n,SS} = \max(0, C^+_{n-1,SS} + Z_n - k_{SS}), \quad C^-_{n,SS} = \min(0, C^-_{n-1,SS} + Z_n + k_{SS}),$$

  where $C^+_{0,SS} = C^-_{0,SS} = 0$, and $k_{SS} > 0$ is an allowance constant. The chart gives a signal when $C^+_{n,SS} > h_{SS}$ or $C^-_{n,SS} < -h_{SS}$, where $h_{SS} > 0$ is a control limit that can be computed by the R-package *spc* for pre-specified ARL_0 and k_{SS} values. Note that this chart cannot accommodate serial data correlation. It also assumes that the original process observations are normally distributed.

- Nonparametric CUSUM chart suggested in Qiu and Li (2011), denoted as QL-CUSUM: This chart is based on data categorization. It cannot accommodate serial data correlation. The IC parameters used in the chart are estimated from the original IC data $\boldsymbol{X}_{IC}$ only (i.e., it is not self-started).

- EWMA chart by Lee and Apley (2011) for monitoring correlated data, denoted as LA-EWMA: This chart assumes that the IC process observations follow an ARMA model $X_n = \frac{\Theta(B)}{\Phi(B)}\varepsilon_n$, for $n \geq 1$, where B is a backward shift operator, $\Phi(B) = 1 -$

$\phi_1 B - \phi_2 B^2 - \cdots - \phi_{r_1} B^{r_1}$ is an autoregressive polynomial of order r_1, $\Theta(B) = 1 - \theta_1 B - \theta_2 B^2 - \cdots - \theta_{r_2} B^{r_2}$ is an moving averaging polynomial of order r_2, and $\{\varepsilon_n\}$ are i.i.d. random errors with the $N(0,1)$ distribution. After the ARMA model is estimated from the IC data $\boldsymbol{X}_{IC}$ with the orders r_1 and r_2 determined by AIC, we define the residuals of the estimated ARMA model to be $\widehat{e}_n = \widehat{\Theta}^{-1}(B)\widehat{\Phi}(B)X_n$, for $n \geq 1$. Then, the charting statistic of LA-EWMA is defined by

$$E_n = (1-\lambda)E_{n-1} + \lambda \widehat{e}_n, \qquad \text{for } n \geq 1,$$

where $E_0 = 0$ and $\lambda \in (0,1]$ is a weighting parameter. The control limits of the chart are chosen to be $\pm L\sqrt{E(\sigma_E^2|\widehat{\boldsymbol{\gamma}})}$, where $E(\sigma_E^2|\widehat{\boldsymbol{\gamma}})$ can be computed by formula (10) in Lee and Apley (2011), $\widehat{\boldsymbol{\gamma}} = (\widehat{\phi}_1, \ldots, \widehat{\phi}_{r_1}, \widehat{\theta}_1, \ldots, \widehat{\theta}_{r_2})^T$ is the vector of the estimated parameters obtained from the IC data $\boldsymbol{X}_{IC}$, and $L > 0$ is a threshold value chosen to reach a given ARL_0 value.

- Simplified G-CUSUM chart, denoted as G1-CUSUM: This chart is the same as G-CUSUM, except that the self-starting mechanism is not implemented (i.e., all the IC parameters are estimated from $\boldsymbol{X}_{IC}$ only).

The following four IC models are considered in the numerical studies. **Case I**: Process observations $\{X_1, X_2, \ldots\}$ are i.i.d. and $N(0,1)$ distributed. **Case II**: Process observations follow the AR(1) model $X_n = 0.5X_{n-1} + \varepsilon_n$, for $n \geq 1$, where $X_0 = 0$ and $\{\varepsilon_n\}$ are i.i.d. random errors with the $N(0,1)$ distribution. **Case III**: Process observations follow the ARMA(2,1) model $X_n = 0.85X_{n-1} - 0.5X_{n-2} + \varepsilon_n - 0.5\varepsilon_{n-1}$, for $n \geq 2$, where $X_0 = X_1 = 0$, and $\{\varepsilon_n\}$ are i.i.d. with the common $\chi^2(3)$ distribution. **Case IV**: Process observations follow the model $X_n = 1.5\xi_n + \varepsilon_n$, where $\{\varepsilon_n\}$ are i.i.d. and $t(4)$-distributed, and $\{\xi_n\}$ is a two-state Markov process with the transition matrix $\begin{pmatrix} 0.75, & 0.25 \\ 0.25, & 0.75 \end{pmatrix}$ and the two states $(0,1)$. Case I is the conventional case considered in the SPC literature. Cases II and III are two different cases with correlated data that follow ARMA models. Case IV considers a serially correlated data scenario that the data correlation cannot be described by an ARMA model. In each of the above four cases, the IC process mean and variance are re-scaled to be 0 and 1, respectively.

3.1 IC performance

We first evaluate the IC performance of the related control charts. In the simulation study, the IC sample size m_0 is fixed at 200, and the nominal ARL_0 value is fixed at 200 for all charts. In the charts G-CUSUM and QL-CUSUM, the number of categories in the data categorization process is fixed at $p = 10$. The allowance constants in the CUSUM charts SS-CUSUM, QL-CUSUM, G-CUSUM and G1-CUSUM are all chosen to be 0.1. The weighting parameter of the chart LA-EWMA is chosen to be $\lambda = 0.05$. The actual ARL_0 values of all five control charts are computed based on 10,000 replicated simulations. The results are presented in Table 1. From the table, it can be seen that the IC performance of SS-CUSUM is good in Case I because all its model assumptions are valid in that case. Its actual ARL_0 values are substantially different from 200 in other three cases because some of its model assumptions (e.g., normality, data independence) are violated in those cases. Both QL-CUSUM and G1-CUSUM do not perform well in all cases because their IC parameter estimates obtained from the original IC data $\boldsymbol{X}_{IC}$ are unreliable due to the relatively small IC data size. The chart LA-EWMA performs well in Cases I and II when its model assumptions are valid, bad in Case III when some model assumptions (e.g., data correlation follows an ARMA model) are valid but the normality assumption is violated, and bad in Case IV when the ARMA data correlation and normality assumptions are both violated. The difference between the actual and nominal ARL_0 values in Cases I and II can be explained by the fact that the ARMA model is estimated from the original IC data $\boldsymbol{X}_{IC}$ whose data size is quite small. As a comparison, the IC performance of the proposed chart G-CUSUM is good in all cases considered.

Table 1: Actual ARL_0 values and their standard errors (in parentheses) of five control charts when their nominal ARL_0 values are fixed at 200 and the IC sample size m_0 is 200.

	SS-CUSUM	QL-CUSUM	LA-EWMA	G-CUSUM	G1-CUSUM
Case I	198 (1.68)	82 (1.61)	177 (3.43)	204 (3.66)	62 (1.27)
Case II	52 (0.36)	23 (0.49)	185 (3.68)	196 (3.52)	64 (1.33)
Case III	755 (7.47)	61 (1.24)	2291 (21.87)	197 (3.57)	64 (1.31)
Case IV	111 (0.88)	39 (1.05)	151 (2.60)	195 (3.44)	60 (1.26)

To see how the IC data size m_0 affects the performance of our proposed chart G-CUSUM, we let m_0 change among 50, 100, 200 and 500, and the remaining setup is kept unchanged

from those in Table 1. The calculated actual ARL_0 values of G-CUSUM are presented in Table 2. It can be seen from the table that the IC performance of G-CUSUM when $m_0 = 50$ is not quite reliable because the differences between the actual and nominal ARL_0 values are more than 10% of the nominal ARL_0 value in Cases II-IV. When m_0 gets larger, the IC performance of G-CUSUM gets more reliable. Actually, the differences between the actual and nominal ARL_0 values are less than or equal to 10% of the nominal ARL_0 value in all cases considered when $m_0 = 100$.

Table 2: Actual ARL_0 values and their standard errors (in parentheses) of G-CUSUM when its nominal ARL_0 values are fixed at 200 and the IC sample size m_0 changes among 50, 100, 200 and 500.

	$m_0 = 50$	100	200	500
Case I	202 (4.07)	205 (3.91)	204 (3.66)	202 (3.57)
Case II	178 (3.59)	186 (3.78)	196 (3.52)	200 (3.42)
Case III	165 (3.26)	182 (3.45)	197 (3.57)	199 (3.55)
Case IV	169 (3.47)	180 (3.55)	195 (3.44)	199 (3.39)

3.2 OC performance

Next, we study the OC performance of the related control charts in cases when $m_0 = 200$ and 1000. In order to make the comparison more meaningful, we intentionally adjust the control limits of the charts SS-CUSUM, QL-CUSUM, LA-EWMA and G1-CUSUM so that their actual ARL_0 values equal 200 in all cases considered. In the simulation study, we assume that a shift of size $\delta\sigma_X$ occurs at the beginning of Phase II monitoring, where δ changes from -1.0 to 1.0 with a step of 0.25 and σ_X is the standard deviation of the IC process observations. Because different control charts have different procedure parameters (i.e., the allowance constant of the four CUSUM-type charts and the weighting parameter of the EWMA-type chart) and their performance may not be comparable if their parameters are set to be the same, we use the following strategy to set up these charts. For a given chart, its parameter is chosen to be the optimal one for detecting a shift of size $0.5\sigma_X$. Namely, the parameter is chosen by minimizing the ARL_1 value of the chart when detecting the shift of size $0.5\sigma_X$ while maintaining the ARL_0 value at 200. This approach for comparing different

control charts has been used in the literature (cf., Qiu and Li 2011). The calculated ARL_1 values of the five charts based on 10,000 replicated simulations when $m_0 = 200$ and 1000 are presented in Figures 1 and 2, respectively. From the plots in the figures, it can be seen that i) all charts perform reasonably well in Case I, ii) charts LA-EWMA and QL-CUSUM perform better than the remaining three charts for detecting small shifts while G-CUSUM performs better for detecting large shifts when $m_0 = 200$, and these three charts perform better than the other two charts with G-CUSUM having a small lead in performance when $m_0 = 1000$ in Case II, iii) G-CUSUM performs the best when $m_0 = 200$ and both G-CUSUM and G1-CUSUM perform well when $m_0 = 1000$ in Case III, and iv) both G-CUSUM and QL-CUSUM perform well when $m_0 = 200$ and G-CUSUM performs the best $m_0 = 1000$ in Case IV. This example shows that the proposed method G-CUSUM performs well in all cases considered, while the remaining charts perform well in some special cases only.

The OC performance of the chart G-CUSUM is affected by the IC data size m_0. In the next example, we let m_0 change among 100, 200, 500, 1,000 and 2,000, and other chart setup remains the same as that in the example of Figure 1. The results are shown in Figure 3. From the plots, it can be seen that i) the larger the value of m_0, the better G-CUSUM performs, ii) the chart is quite stable in most cases when $m_0 \geq 500$, and iii) it seems that its OC performance is reasonably stable in all cases considered when $m_0 \geq 1,000$.

In the above examples, the allowance constant k of G-CUSUM is chosen to be the optimal ones for detecting the shift of $0.5\sigma_X$ in Cases I-IV. Next, we study the impact of k on the performance of G-CUSUM by changing the k value among $\{0.001, 0.005, 0.01, 0.05, 0.1\}$ and keeping the other chart setup to be the same as that in Figure 1. The results are shown in Figure 4. From the plots, we can see that the OC performance of G-CUSUM is stable in all cases considered when $k \leq 0.01$.

The chart G-CUSUM is based on data categorization and the number of categories is fixed at $p = 10$ in all examples discussed above. To study the impact of p on the OC performance of G-CUSUM, we let p change among 2, 5, 10, and 15 in the next example, and other chart setup remains unchanged from that in the example of Figure 1. The results are shown in Figure 5. From the plots, it can be seen that the chart performance is stable when $p \geq 5$ in most cases considered, and its performance could not be improved much when $p \geq 10$.

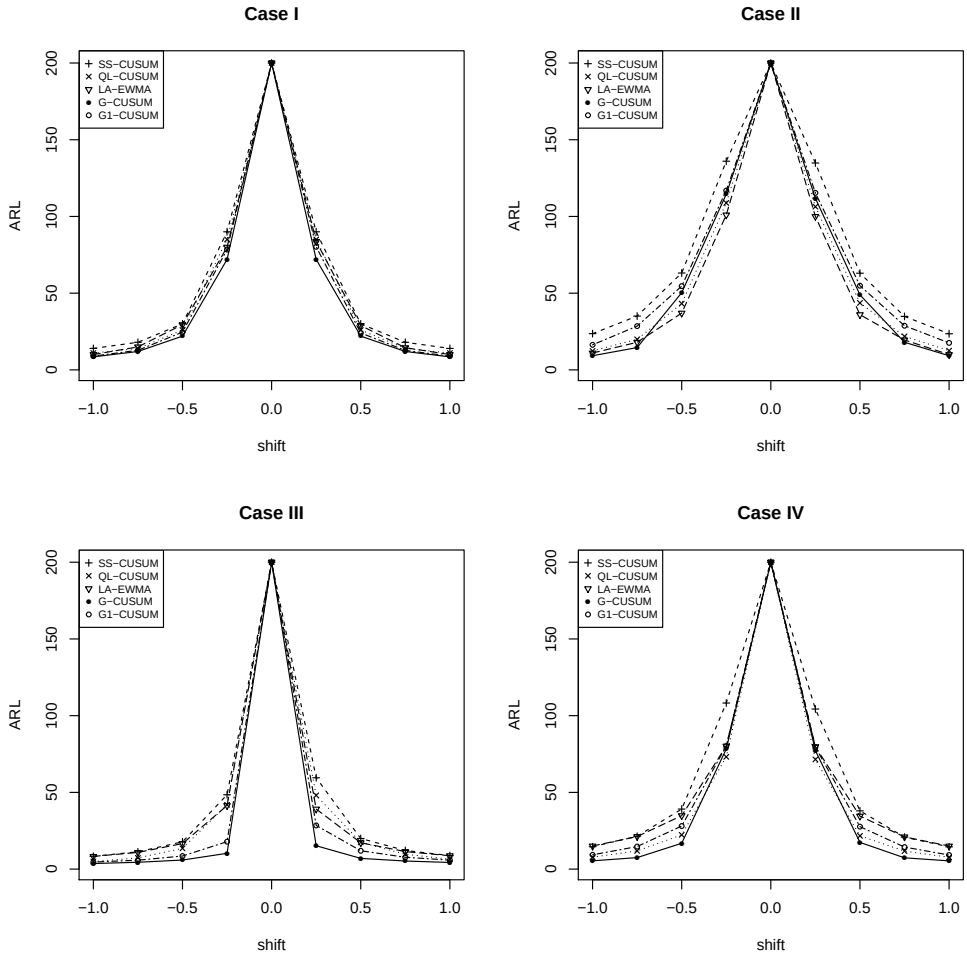

Figure 1: ARL_1 values of five control charts when ARL_0 is set at 200, $m_0 = 200$, and the procedure parameters are chosen to be the optimal ones for detecting a shift of the size $0.5\sigma_X$.

In the next example, we study the joint impact of m_0, p and b_{max} on the OC performance of G-CUSUM. In the setup of Figure 1, we let m_0 change between 200 and 1000, p change between 2 and 10, and b_{max} change between 5 and 10. In each of the eight combinations of m_0, p and b_{max}, the ARL_1 values of G-CUSUM are calculated in the same way as that in Figure 1 that ARL_0 is set at 200 and the allowance constant k is chosen to minimize the ARL_1 value for detecting the shift of $0.5\sigma_X$. The results in Cases I-IV are shown in Figure 6. From the plots in the figure, it can be seen that: i) the chart performance is similar when b_{max} changes from 5 to 10 in all cases considered, ii) the chart performs much better when p equals 10, compared to its performance when p equals 2, and iii) the overall performance of the chart is improved when m_0 increases from 200 to 1000, although the improvement

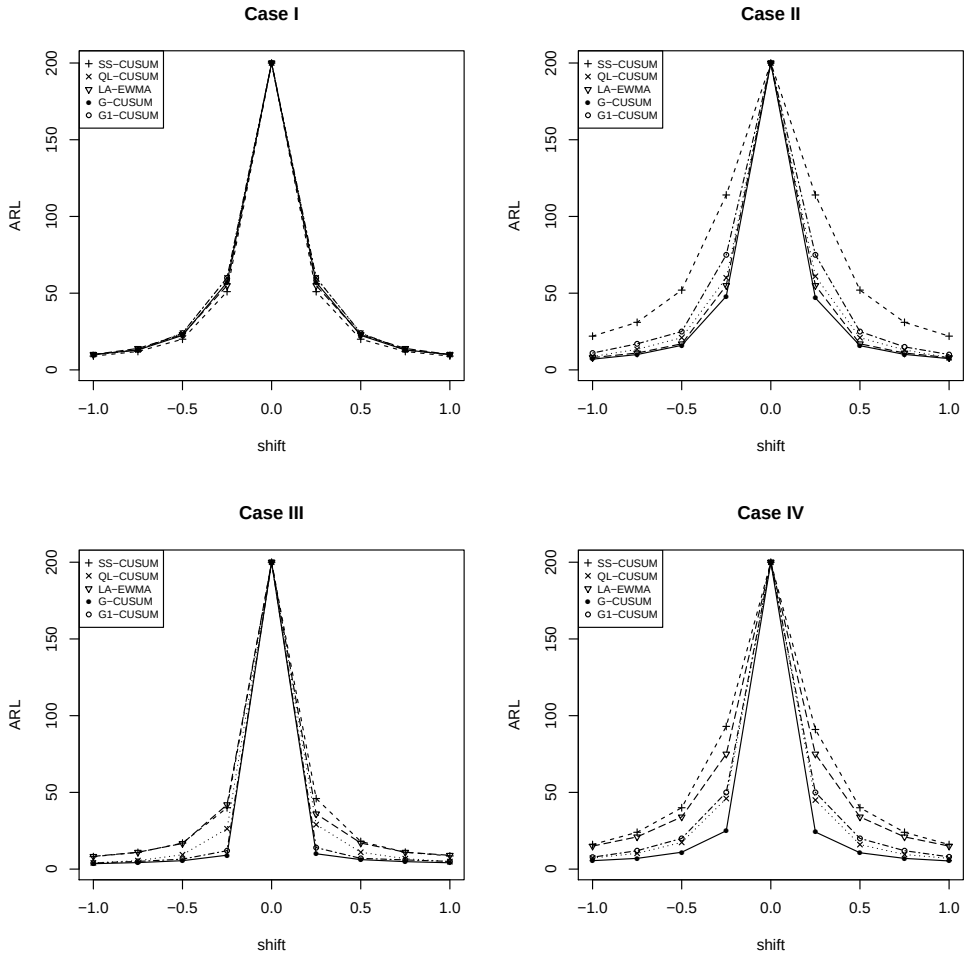

Figure 2: ARL_1 values of five control charts when ARL_0 is set at 200, $m_0 = 1000$, and the procedure parameters are chosen to be the optimal ones for detecting a shift of the size $0.5\sigma_X$.

is quite small in Cases I and III when $p = 10$. This example further confirms the results obtained in the previous examples and our recommended guidelines given in Section 2.3.

4 A Real Data Application

In this section, we illustrate the proposed control chart using a real-data example about the daily exchange rates between Korean Won and US Dollar in the period between March 28, 1997 and December 02, 1997. During this time period, the daily exchange rates were quite stable early on and became unstable starting from early August, due to the global financial

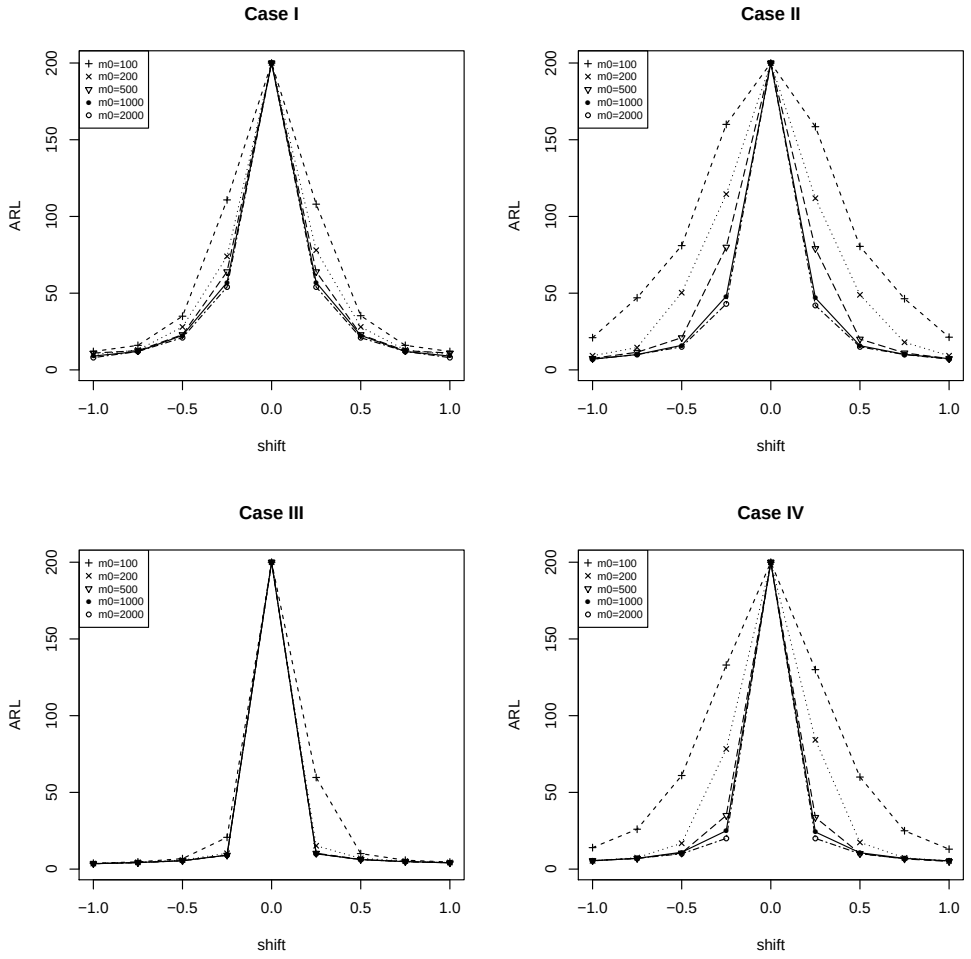

Figure 3: ARL_1 values of G-CUSUM when ARL_0 is set at 200, m_0 changes among 100, 200, 500, 1,000 and 2,000, and the other chart setup remains the same as that in the example of Figure 1.

crisis. This can be seen from Figure 7, where 173 daily exchange rates (Won/Dollar) observed in that period are shown.

We then apply the related control charts considered in the previous section to this dataset, by using the first 90 observations as the initial IC data (or Phase I data) and the remaining observations for Phase II online monitoring. In Figure 7, the Phase I and Phase II data are separated by a dashed vertical line. To take a closer look at the initial IC data, the Durbin-Watson test for testing autocorrelation gives a p-value of 2.2×10^{-16}, which provides a strongly significant evidence that the initial IC data are correlated. The Shapiro test for checking normality of the IC data gives a p-value of 1.965×10^{-4}, implying that the

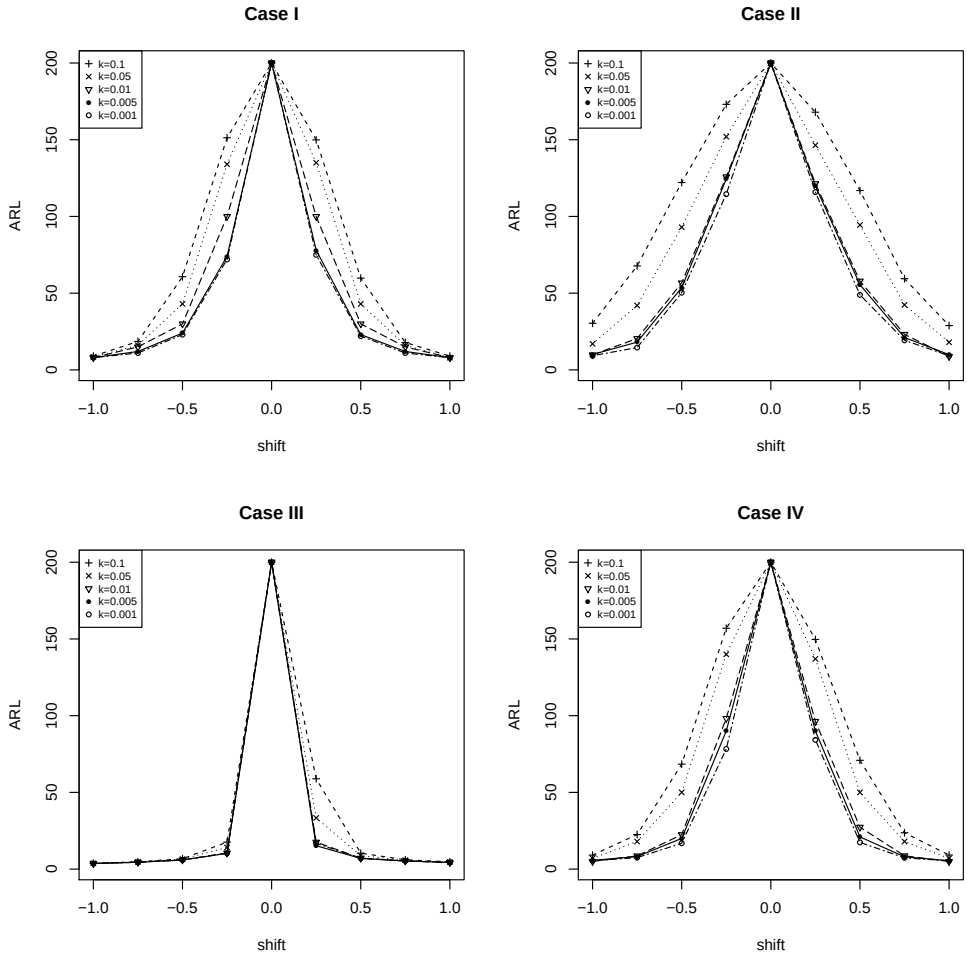

Figure 4: ARL_1 values of G-CUSUM when ARL_0 is set at 200, $m_0 = 200$, k changes among 0.001, 0.005, 0.01, 0.05, and 0.1, and the other chart setup remains the same as that in the example of Figure 1.

IC data are significantly non-normal. To check whether an ARMA model is appropriate for describing the data autocorrelation, we fit an ARMA model to the centralized Phase I data and use AIC for choosing its orders. Then, the resulting model is the following ARMA(1,0) model $X_j = 0.9008X_{j-1} + \varepsilon_j$. Remember that if this ARMA model provides a good fit to the centralized Phase I data, then the residuals should be approximately normally distributed with mean 0. The Q-Q plot of the residuals is shown in Figure 8, from which it can be seen that the distribution of the residuals is quite far away from normal. Thus, the fitted ARMA model is inappropriate for describing the data autocorrelation in the Phase I exchange rate data, and all existing methods based on ARMA models are inappropriate to use in this example either.

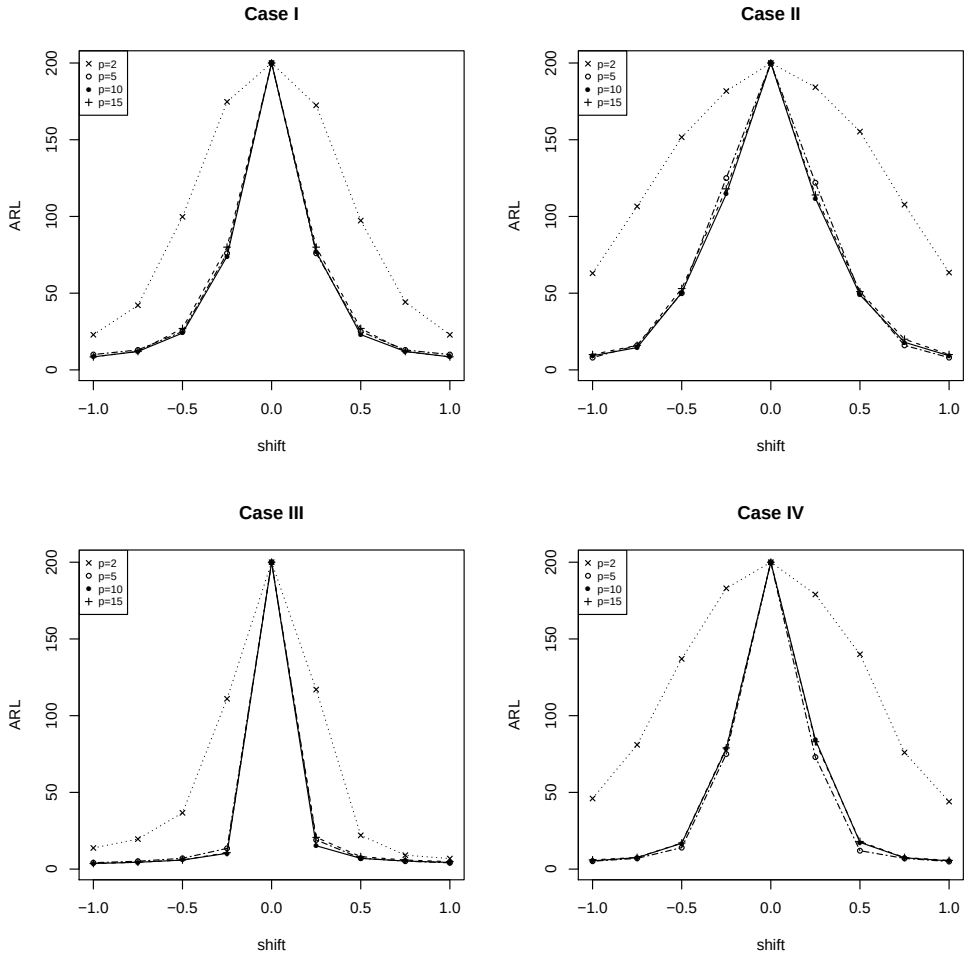

Figure 5: ARL_1 values of G-CUSUM when ARL_0 is set at 200, $m_0 = 200$, p changes among 2, 5, 10, and 15, and the other chart setup remains the same as that in the example of Figure 1.

When the nominal ARL_0 value is fixed at 200, the allowance constants of the four CUSUM charts are all chosen to be 0.1, and the weighting parameter in LA-EWMA is chosen to be $\lambda = 0.05$, the five control charts are shown in Figure 9, where the dashed horizontal lines denote their control limits. From the plots, the G-CUSUM, G1-CUSUM, SS-CUSUM, QL-CUSUM, and LA-EWMA charts give signals at the 9th, 24th, 36st, 22th, and 29th Phase II observations, respectively. Therefore, the signal by G-CUSUM is the earliest one in this example, and the control charts confirm that the exchange rate between Korean Won and US Dollar does have a distributional shift during an early stage of Phase II process monitoring.

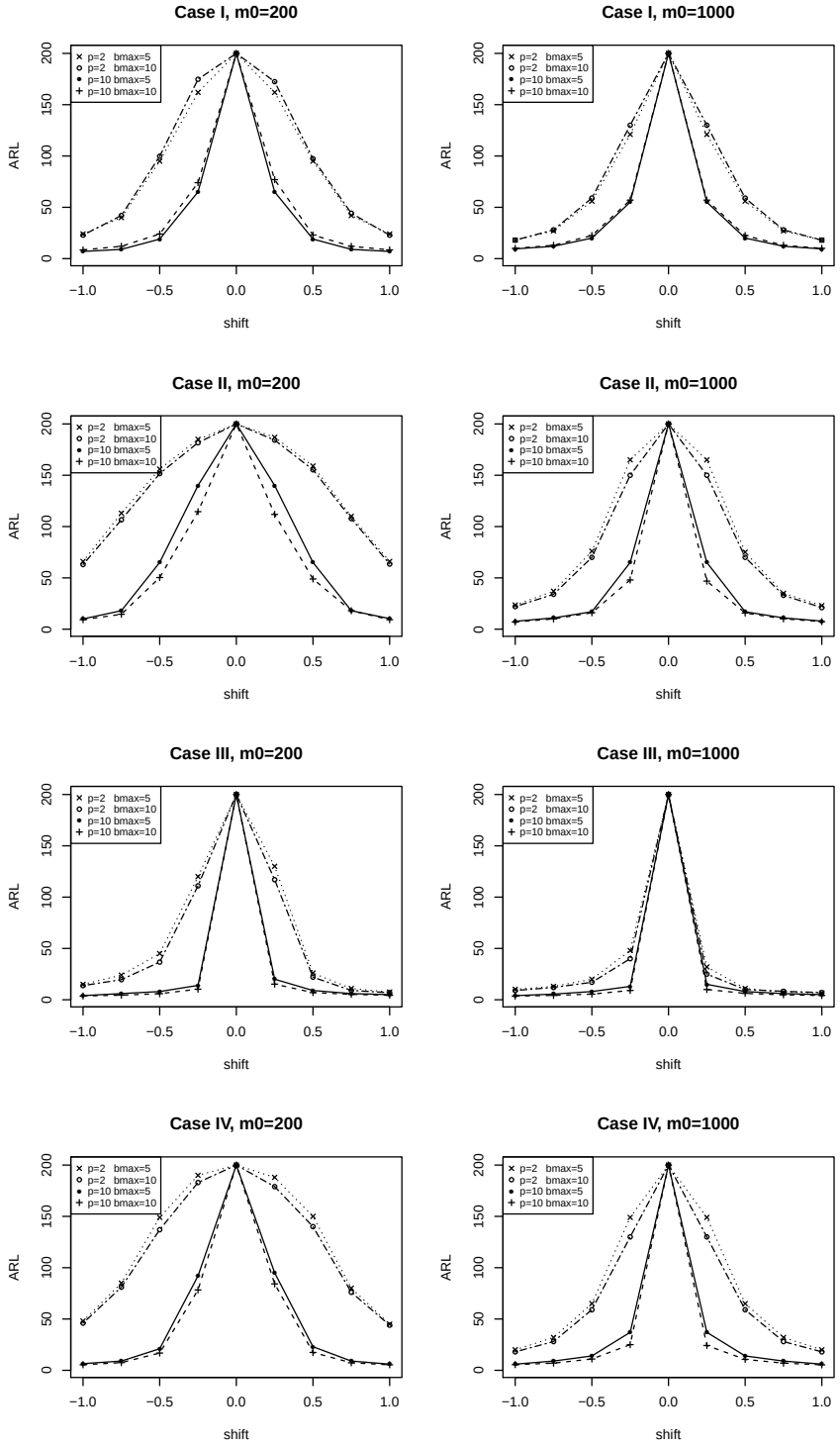

Figure 6: ARL_1 values of G-CUSUM when ARL_0 is set at 200, $m_0 = 200$ or 1000, $p = 2$ or 10, $b_{max} = 5$ or 10, and the other chart setup remains the same as that in the example of Figure 1.

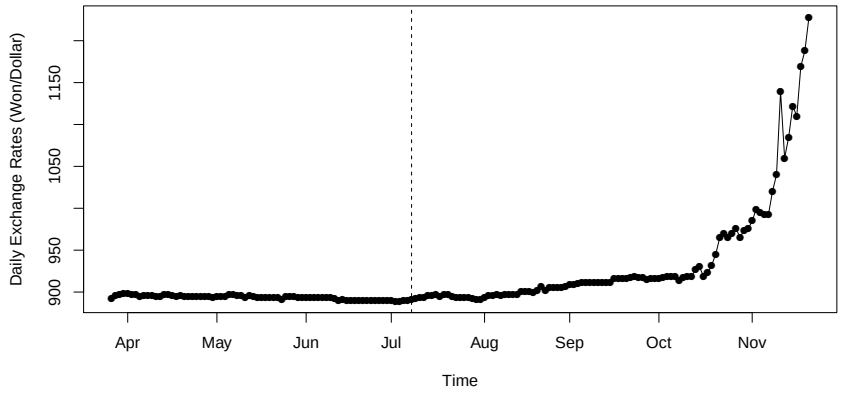

Figure 7: Original observations of the exchange rate data between Korean Won and US Dollar during March 28 and December 02, 1997. The vertical dashed line separates the initial IC data from the Phase II observations.

5 Concluding Remarks

We have proposed a general charting scheme for monitoring serially correlated process observations with short-memory dependence and nonparametric IC distributions. This charting method only requires a small to moderate initial IC dataset and a quite flexible serial data correlation structure that data correlation is homogeneous over time and the correlation between two observations is weaker when the observation times are farther away. Numerical studies show that it works well in different cases. Because of its great flexibility, it should be able to provide a powerful tool for many process monitoring applications. It is our believe that the already flexible homogeneous data correlation assumption can be further weakened. One possibility is to estimate the covariance function $\gamma(s)$ (cf., its definition in the first paragraph of Section 2) based on a certain amount of previous observations that is immediately before the current time point n only. In that case, the covariance function can be assumed time-varying, instead of homogeneous in time. But, the estimated covariance function could have relatively large variability. Also, the control limit h of the proposed chart G-CUSUM is currently determined by the initial IC dataset alone. The chart can be improved by updating the value of h every time when the current observation X_n is combined with the previous IC data. But, the computation involved will be more demanding. These topics will be studied in our future research.

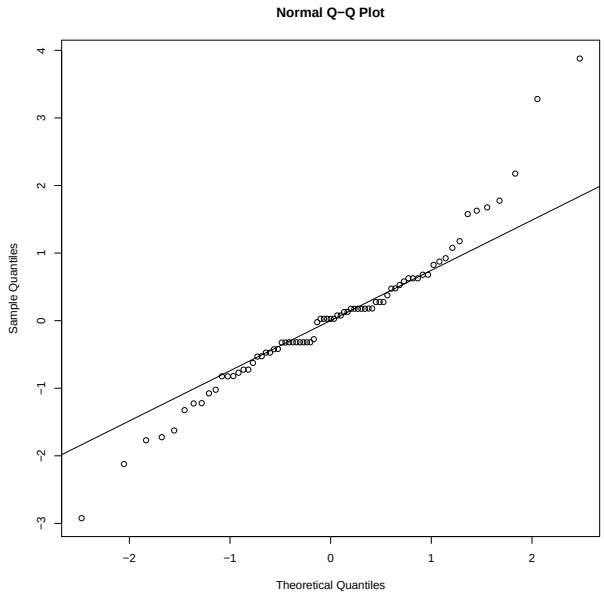

Figure 8: Q-Q plot of the residuals of the ARMA(1,0) model fitted from the Phase I exchange rate data.

Acknowledgments: The authors appreciate the constructive comments and suggestions from the focus issue editor, Professor Judy Jin, and the two referees, which greatly improved the quality of the paper. This research was finished during the one-year visit of the first author at the Department of Biostatistics at the University of Florida.

Author Biosketches

Wendong Li is currently a PhD student of the School of Statistics at the East China Normal University in Shanghai, China. He visited the Department of Biostatistics of the University of Florida as a visiting student for one year during October 2017 - October 2018. His major research areas include statistical process control, quality management, change-point detection, and many different applications.

Peihua Qiu received his Ph.D. in statistics from the Statistics Department at the University of Wisconsin at Madison in 1996. He worked as a senior research consulting statistician of the Biostatistics Center at the Ohio State University during 1996-1998. He then worked as an assistant professor (1998-2002), an associate professor (2002-2007), and a full professor (2007-2013) at the School of Statistics at the University of Minnesota. He is an

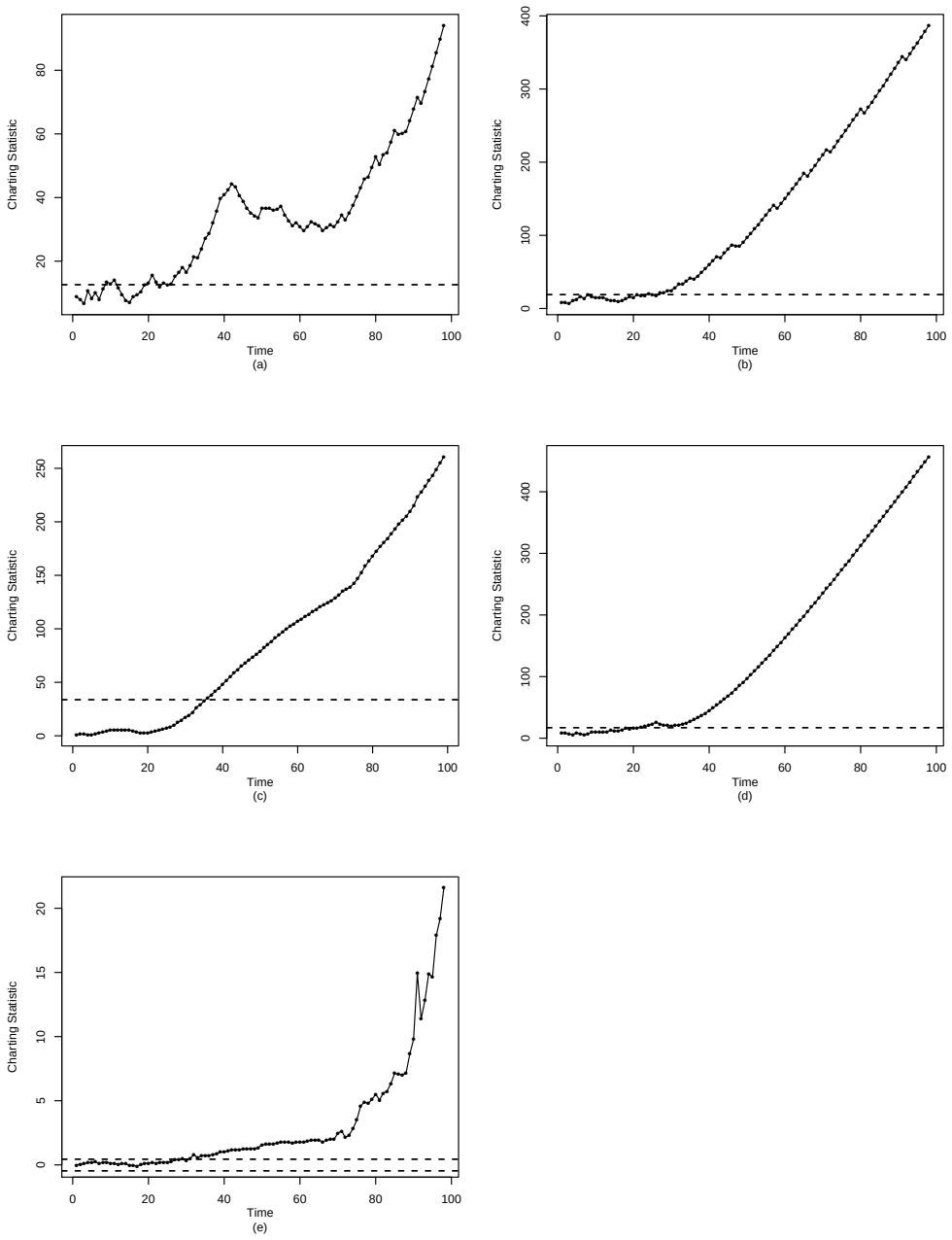

Figure 9: Control charts G-CUSUM (plot (a)), G1-CUSUM (plot (b)), SS-CUSUM (plot (c)), QL-CUSUM (plot (d)) and LA-EWMA (plot (e)) when they are applied to the exchange rate data shown in Figure 7. The horizontal dashed lines are the control limits.

elected fellow of the American Statistical Association, an elected fellow of the Institute of Mathematical Statistics, an elected member of the International Statistical Institute, a senior member of the American Society for Quality, and a lifetime member of the International Chinese Statistical Association. He served as associate editor for *Journal of the American Statistical Association* (2006-2012), *Biometrics* (2011-2012), *Technometrics* (2007-2012), and *Statistical Papers* (2011-2012), and guest co-editor for *Multimedia Tools and Applications*, and *Quality and Reliability Engineering International*. He was the editor-elect (2013) and editor (2014-2016) of *Technometrics*. He is currently the associate editor of *Surgery* and *Quality Engineering*, and the founding chair of the Department of Biostatistics at the University of Florida.

Peihua Qiu has made substantial contributions in the areas of jump regression analysis, image processing, statistical process control, survival analysis and disease screening and surveillance. So far, he has published over 100 research papers, many of which appeared in top journals, including *Technometrics, Journal of the American Statistical Association, Annals of Statistics, Annals of Applied Statistics, Journal of the Royal Statistical Society (Series B), Biometrika, Biometrics, IEEE Transactions on Pattern Analysis and Machine Intelligence*, and *IIE Transactions*. His research monograph titled *Image Processing and Jump Regression Analysis* (2005, Wiley) won the inaugural Ziegel prize in 2007 for its contribution in bridging the gap between jump regression analysis in statistics and image processing in computer science. His second book titled *Introduction to Statistical Process Control* was published in 2014 by Chapman & Hall/CRC.

References

Agresti, A. (2012), *Categorical Data Analysis (3rd edition)*, New York: John Wiley & Sons.

Apley D.W., and Lee, H.C. (2003), "Design of exponentially weighted moving average control charts for autocorrelated processes with model uncertainty," *Technometrics*, **45**, 187–198.

Apley D.W., and Lee, H.C. (2008), "Robustness comparison of exponentially weighted moving-average charts on autocorrelated data and on residuals," *Journal of Quality Technology*, **40**, 428–447.

Apley D.W., and Tsung, F. (2002), "The autoregressive T^2 chart for monitoring univariate autocorrelated processes," *Journal of Quality Technology*, **34**, 80–96.

Box, G.E.P., Jenkins, G.M., and Reinsel, G.C. (2013), *Time series analysis: Forecasting and Control,* New York: John Wiley & Sons.

Chakraborti, S., van der Laan, P. and Bakir, S.T. (2001), "Nonparametric control charts: an overview and some results," *Journal of Quality Technology*, **33**, 304–315.

Chakraborti, S., Qiu, P., and Mukherjee, A. (2015), "Editorial to the special issue: Nonparametric statistical process control charts," *Quality and Reliability Engineering International*, **31**, 1–2.

Chatterjee, S., and Qiu, P. (2009), "Distribution-free cumulative sum control charts using bootstrap-based control limits," *The Annals of Applied Statistics*, **3**, 349–369.

Hawkins, D.M. (1987), "Self-starting CUSUM charts for location and scale," *Journal of the Royal Statistical Society. Series D (The Statistician)*, **36**, 299–316.

Hawkins, D.M., and Olwell, D.H. (1998), *Cumulative Sum Charts and Charting for Quality Improvement*, New York: Springer-Verlag.

Lee, H. C., and Apley, D. W. (2011), "Improved design of robust exponentially weighted moving average control charts for autocorrelated processes," *Quality and Reliability Engineering International*, **27**, 337–352.

Li, J. (2017), "Nonparametric adaptive CUSUM chart for detecting arbitrary distributional changes," arXiv:1712.05072.

Li, J., and Qiu, P. (2016), "Nonparametric dynamic screening system for monitoring correlated longitudinal data," *IIE Transactions*, **48**, 772–786.

Li, J., Zhang, X., and Jeske, D.R. (2013), "Nonparametric multivariate CUSUM control charts for location and scale changes," *Journal of Nonparametric Statistics*, **25**, 1–20.

Loredo, E., Jearkpaporn, D., and Borror, C. (2002), "Model-based control chart for autoregressive and correlated data," *Quality and Reliability Engineering International*, **18**, 489–496.

Montgomery, D.C. (2012), *Introduction to Statistical Quality Control*, New York: John Wiley & Sons.

Mukherjee, A., Graham, M.A., and Chakraborti, S. (2013), "Distribution-free exceedance CUSUM control charts for location," *Communications in Statistics - Simulation and Computation*, **42**, 1153–1187.

Qiu, P. (2008), "Distribution-free multivariate process control based on log-linear modeling," *IIE Transactions*, **40**, 664–677.

Qiu, P. (2014), *Introduction to statistical process control,* Boca Raton, FL: Chapman Hall/CRC.

Qiu, P. (2018), "Some perspectives on nonparametric statistical process control," *Journal of Quality Technology*, **50**, 49–65.

Qiu, P., and Hawkins, D.M. (2001), "A rank based multivariate CUSUM procedure," *Technometrics*, **43**, 120–132.

Qiu, P., and Hawkins, D.M. (2003), "A nonparametric multivariate CUSUM procedure for detecting shifts in all directions," *JRSS-D (The Statistician)*, **52**, 151–164.

Qiu, P., and Li, Z. (2011), "On nonparametric statistical process control of univariate processes," *Technometrics*, **53**, 390–405.

Qiu, P., Li, W., and Li, J. (2019), "A new process control chart for monitoring short-range serially correlated data," *Technometrics*, DOI:10.1080/00401706.2018.1562988.

Runger, G. (2002), "Assignable causes and autocorrelation: control charts for observations or residuals?" *Journal of Quality Technology*, **34**, 165–170.

Vermaat, M.B., Does, R., and Bisgaard, S. (2008), "EWMA control chart limits for first- and second-order autoregressive processes," *Quality and Reliability Engineering International*, **24**, 573–584.

Wardell, D.G., Moskowitz, H., Plante, R.D. (1994), "Run-length distributions of special-cause control charts for correlated processes," *Technometrics*, **36**, 3–17.

Zhang, N. F. (1998), "A statistical control chart for stationary process data," *Technometrics*, **40**, 24–38.

Zou, C., Wang, Z., and Tsung, F. (2012), "A spatial rank-based multivariate EWMA control chart," *Naval Research Logistics*, **59**, 91–110.